PCCP

Accepted Manuscript

ROYAL SOCIETY OF CHEMISTRY

www.rsc.org/pccp

PCCP

RSCPublishing

ARTICLE

Insights into the Cr(III) catalysed isomerization mechanism of glucose to fructose in the presence of water using *ab initio* molecular dynamics

Cite this: DOI: 10.1039/xoxxoooooox

Received ooth January 2012,
Accepted ooth January 2012

DOI: 10.1039/xoxxoooooox

www.rsc.org/

Samir H. Mushrif,*[a] Jithin J. Varghese[a] and Dionisios G. Vlachos[b]

The mechanism of glucose ring opening and isomerization to fructose, catalyzed by the Lewis acid catalyst $CrCl_3$ in the presence of water, is investigated using Car–Parrinello molecular dynamics with metadynamics. Minimum energy pathways for the reactions are revealed and the corresponding free energy barriers are computed. Addition of glucose replaces two water molecules in the active $[Cr(H_2O)_5OH]^{+2}$ complex, with two hydroxyl groups of glucose taking their place. Ring opening and isomerization reactions can only proceed if the first step involving the deprotonation of glucose is accompanied by the protonation of the OH^- group in the partially hydrolyzed metal center ($[Cr(C_6H_{12}O_6)(H_2O)_3OH]^{+2}$ ➔ $[Cr(C_6H_{11}O_6)(H_2O)_4]^{+2}$). This provides further evidence that the partially hydrolyzed $[Cr(H_2O)_5OH]^{+2}$ is the active species catalyzing ring opening and isomerization reactions and that unhydrolysed Cr^{+3} may not be able to catalyze the reactions. After the ring opening, the isomerization reaction proceeds via deprotonation, followed by hydride shift and the back donation of the proton from the metal complex to the sugar. Water molecules outside the first coordination sphere of the metal complex participate in the reaction for mediating the proton transfer. Hydride shift in the isomerization is the overall rate limiting step with a free energy barrier of 104 kJ/mol. The simulation computed barrier is in agreement with experiments.

Introduction

As a renewable source for hydrocarbons, biomass is a promising candidate.[1,2] Carbohydrates constitute more than 75% of the vast amount of biomass produced by nature and barely 5% of them are consumed in food and non–food sectors.[3] For the utilization of biomass, it is imperative to develop processes that can convert these carbohydrates into useful chemicals and fuels. However, carbohydrates are highly functional molecules owing to the presence of oxygen. Hence, it is vital to selectively remove the oxygenated groups so that they can be transformed into a variety of chemical intermediates in fine chemicals, polymers, plastics and fuels sectors. 5-hydroxymethyl-furfural (HMF) and its 2,5-disubstituted furan derivatives are such key building-block molecules, currently derived from petrochemicals. Dehydration of fructose to HMF in aqueous media has been successfully performed by Dumesic and coworkers.[4,5] However, economic analysis of the process has shown that the cost of the product HMF is most sensitive to the initial cost of fructose.[6] Hence, it becomes crucial to efficiently convert glucose to fructose. Glucose is the monomer unit of cellulose and a readily available and less expensive sugar.

Isomerization of glucose to fructose is the largest immobilized biocatalytic process worldwide for the production of high fructose corn syrup. However, enzymatic processes face several limitations:[7] (1) they require extremely high purity of glucose; (2) they are slow and expensive; (3) the enzyme catalyst goes through an irreversible decay; and (4) they can only operate within a very narrow temperature and pH (basic) range. This makes a single pot conversion of glucose to HMF (and subsequently to levulinic acid, if γ–valerolactone is the desired product) difficult, as after the isomerization, fructose needs to be dehydrated to HMF in an acidic environment at temperatures higher than 90 °C. Alternate approaches to this process were proposed by Davis and co-workers using the zeolite Sn-beta, a heterogeneous Lewis acid catalyst,[8] and recently by Vlachos and co-workers using $CrCl_3$, a homogeneous Lewis acid catalyst.[9-12] They also demonstrated promising results for a "single pot" conversion of glucose to fructose to HMF by carrying in tandem isomerization and dehydration reactions by combining Lewis and Brønsted acid

catalysts in aqueous media. In general, a heterogeneous catalyst would be a preferred choice since it is easy to separate and reuse. However, the dehydration reaction of fructose to HMF and rehydration of HMF to levulinic acid are associated with side reactions that lead to the formation of soluble polymers and insoluble humins. These by-products can deactivate the catalyst by clogging its pores. In addition to Cr (III), various metals (as salts) like Al (III), Zn (II), Sn (IV) carry out this chemistry[13-18] with the highest yield of HMF from glucose (~60%) obtained from Al (III) and Cr (III). Al (III) is less active than Cr (III) for glucose isomerization to fructose.[11]

In the homogeneously catalyzed glucose to HMF conversion, it was thought that the metal ion was the active Lewis acid center for isomerization and that the addition of an inorganic acid like HCl, provided the Brønsted acidity for the dehydration of fructose to HMF. Using a speciation model together with kinetic experiments for $CrCl_3$, it was recently suggested[11] that the active species might not be hexahydrated Cr^{+3}, but the partially hydrolyzed $[Cr(H_2O)_5OH]^{+2}$ complex. Additionally, even without the addition of any inorganic acid, the hydrolysis of Cr^{+3} by water molecules releases a proton and reduces the pH of the medium,[11, 19, 20] providing Brønsted acidity to drive fructose dehydration.

$$[Cr(H_2O)_6]^{+3} + H_2O \leftrightarrow [Cr(H_2O)_5OH]^{+2} + H_3O^+$$

Car–Parrinello molecular dynamics (CPMD) simulations and EXAFS analysis suggest that Cr^{+3} remains coordinated with 6 oxygens of water in the absence of glucose. Upon the addition of glucose, two oxygen atoms of the hydroxyl groups in glucose replace 2 water molecules within the inner coordination sphere. The metal center is then coordinated with 3 water molecules, one OH^-, and two oxygen atoms of the glucose molecule. It is hypothesized that this complexation of glucose with the active $[Cr(H_2O)_5OH]^{+2}$ species is the first step in the isomerization of glucose to fructose. Similar behaviour is expected for other metals like Al, Zn, and Sn. Importantly, isotopic labelling and kinetic isotope effects indicate that the mechanism of glucose isomerization in Cr–containing solution could be analogous to that of heterogeneous Sn-beta zeolite and is an intramolecular hydride transfer from the C_1 to the C_2 carbon.[21] This provides promise for understanding homogeneous Lewis acid isomerization chemistry and to extend the findings to heterogeneous catalysts.

To gain a molecular level understanding of $CrCl_3$ catalyzed isomerization of glucose to fructose and to explain the catalytic role of the partially hydrolyzed metal center in the reaction, we investigate the mechanism of glucose isomerization to fructose, catalyzed by the active $[Cr(H_2O)_5OH]^{+2}$ species, in the presence of water, using *ab initio* molecular dynamics. Simulations are performed with explicit, quantum mechanically treated water molecules, glucose, and the active catalyst species. Since isomerization is preceded by glucose ring opening and $[Cr(H_2O)_3OH]^{+2}$ is also believed to catalyze the ring opening process, the catalytic transformation of closed ring glucose/glucopyranose to its open chain form is also studied. Reaction mechanisms, minimum free energy pathways and the corresponding free energy barriers in ring opening and isomerization are reported. The role of OH^- group, coordinated with Cr in $[Cr(H_2O)_5OH]^{+2}$, in reducing the free energy barrier of the ring opening and the isomerization reaction is discussed. Participation of water in the reaction chemistry is demonstrated. To the best of our knowledge, this is the first comprehensive paper reporting the molecular level mechanism and energetics of metal salt catalyzed glucose isomerization reaction while considering the dynamics of explicit water.

Computational Methods

All the simulations were performed using the CPMD package; version 3.15.1.[22] The CPMD package implements the Car–Parrinello scheme[23] for *ab initio* molecular dynamics calculations. The first–principles calculations were performed using the planewave–pseudopotential implementation of Kohn–Sham density functional theory.[24] The Troullier–Martins pseudopotential[25] with the Perdew–Burke–Ernzerhof generalized gradient approximation[26] was used for all the atoms in the simulation system. Only the Γ-point was used for integration over the Brillouin zone in the reciprocal space. An energy cut–off of 100 Ryd. was used. The simulation system contained one Cr^{+3}, an OH^- ion, 2 Cl^- ions, a pyranosic glucose molecule and 11 water molecules. 3 of the water molecules were directly coordinated with the metal and 8 water molecules were out of the inner coordination sphere. Extra water molecules were taken to allow the possibility of water mediated proton transfer during reaction steps. The size of the simulation cell was 18 ×18 ×18 $Å^3$ and more than 3 Å space between the outermost atom and the border of the simulation cell was kept to avoid any artefacts, as suggested in the CPMD manual. Unlike the condensed phase environment, a smaller simulation system was implemented to render these expensive calculations tractable. However, the rate determining step in the reaction was studied in the presence of 124 explicit water molecules, under experimental density. Each and every atom in the simulation system was treated quantum mechanically. Calculations were performed with spin polarization on and the ground state spin multiplicity of the system was taken as 4. The metal cation is coordinated with OH^-, 3 water molecules and two oxygen atoms of the hydroxyl groups of glucose, and Cl^- ions are not present within the first coordination sphere of the metal (*cf.* Scheme 1).

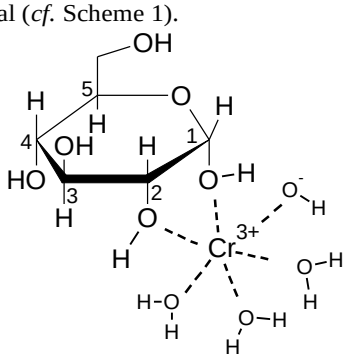

Scheme 1 Octahedral coordination of Cr^{+3} with glucose, OH^- and 3 water molecules. Carbon atoms in glucose are numbered from 1 to 6.

This is in agreement with EXAFS data that suggests that the metal center is coordinated with 6 oxygen atoms in an octahedral fashion.[11] Our previous work[11] on CPMD simulations of the metal coordination with glucose, water and OH^- also suggested that the coordination of glucose replaces two water molecules in $[Cr(H_2O)_5OH]^{+2}$. As this particular arrangement of Cr with glucose and water is also believed to be the first step in glucose ring opening and thus isomerization, we chose this as our starting configuration (*cf.* Scheme 1). In the cascade of reactions including glucose to fructose isomerization followed by fructose dehydration to HMF,[11] the concentration of this species can be low; thus, our simulations here focus on the potentially active species in the local environment of water and glucose only, rather than simulating all Cr-containing species. It has to be noted that there exists a dynamic equilibrium between OH^- and water molecules attached to Cr^{+3}. During the CPMD run, we observed that the OH^- group abstracts a proton from a neighbouring water molecule coordinated with Cr^{+3}, thus becoming a water molecule itself and making the original water molecule an OH^-. Nosé-Hoover chain thermostat was used for controlling ionic and electronic temperatures. The frequency for the ionic thermostat was set to 1800 cm^{-1} (characteristic of a C–C bond vibration frequency) and for the electron thermostat to 10000 cm^{-1}. The fictitious electron mass parameter in CPMD was set to 400 a.u. Short molecular dynamics runs without the thermostat were performed to obtain an approximate value around which the fictitious electronic kinetic energy oscillates. Based on the observations from these runs, a value of 0.01 a.u. was chosen for the electronic kinetic energy. The timestep of a single molecular dynamics step was set to 0.0964 fs. Geometry optimization was performed on the system before molecular dynamics and the system was equilibrated for 1 ps. Energies, including the fictitious electronic kinetic energy were monitored throughout the simulation to ascertain that the system does not deviate from the Born–Oppenheimer surface during the molecular dynamics simulation. Molecular dynamics trajectories were visualized using the VMD software.[27]

CPMD simulations are computationally expensive and hence it is not feasible to run a simulation for experimental reaction timescales. The metadynamics technique[28-30] was thus implemented in conjunction with CPMD to accelerate the dynamics and avoid being trapped in deep minima of the energy surface. It allows the construction of multidimensional free energy surface along selected reaction coordinates. This technique, as described by Laio and Gervasio,[29] is based on "filling up" the free energy surface by dropping potentials at small time intervals in the coordinate space of interest. The flattening of the free energy surface thus helps the system to overcome the activation energy barriers. The details of how metadynamics is implemented by extending the Car–Parrinello Lagrangian in CPMD can be found in the literature.[28] The collective variables (or reaction coordinates) implemented to simulate the glucose ring opening and isomerization reactions are described in the respective sections. The parameters in metadynamics were not optimized for the system studied in this paper, but general guidelines provided in the literature[31, 32] were followed. The height of the metadynamics potential was kept fixed at 1.25 kJ. Analogous to the original Car–Parrinello scheme, the dynamics of the collective variables were separated from the ionic and fictitious electronic motion by choosing an appropriate value for the fictitious mass of the collective variables. The temperature of the collective variables is set to 375 K (same as the physical temperature of the system) and is controlled in a window of ± 200 K using velocity rescaling. A sample input file of the CPMD–metadynamics simulation in this work is provided as supporting information.

Results and Discussion

Glucose Ring Opening

The first step in glucose isomerization is the opening of the pyranosic ring (*cf.* Scheme 2). More than 99.5% of glucose exists in water in the pyranosic form, and the six membered pyranosic ring is coordinated with $[Cr(H_2O)_3OH]^{+2}$, as shown in Scheme 1, and as suggested earlier using EXAFS data and CPMD calculations.[11] Hence, this was taken as the starting structure for simulating the ring opening step. One picosecond of CPMD simulation without metadynamics was performed on the starting configuration to allow the system to equilibrate at finite temperature. During equilibration, it was observed that the hydroxyl group of the C_1 carbon of the glucose ring gets deprotonated and loses the proton to a neighbouring water molecule that is not in the first coordination sphere of the metal. It has to be noted that this reactive event of deprotonation was captured within a small timescale during the CPMD simulation without any metadynamics acceleration. All other steps in glucose ring opening and isomerization require metadynamics acceleration.

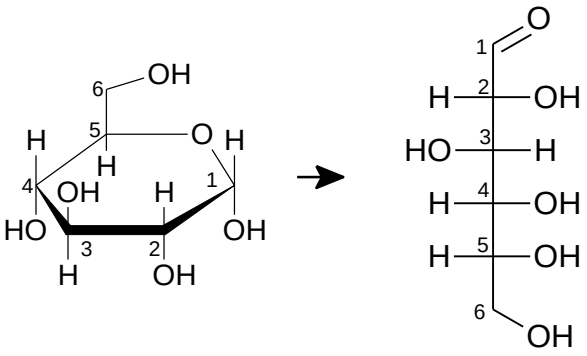

Scheme 2 Ring opening of glucose molecule. Carbon atoms are labelled from 1 to 6.

Glucose ring opening involves the cleavage of C_1–O (ring oxygen) bond and the transfer of 'H' from the hydroxyl group of C_1 to the ring oxygen (*cf.* Scheme 2). However, two different pathways are possible for the 'H' transfer. One does not involve the OH^- group on the metal center and the proton which is already removed from the C_1 hydroxyl group is transferred to the ring oxygen, via water mediated proton transfer (*cf.* Fig.

1a). The other entails the protonation of the OH^- group in $[Cr(H_2O)_3OH]^{+2}$, thus forming glucose coordinated $[Cr(H_2O)_4]^{+3}$ as an intermediate that later transfers the proton to the ring oxygen (direct transfer or water mediated) as the C_1–ring oxygen bond cleaves (*cf.* Fig. 2a).

To find the minimum energy pathway for glucose ring opening and to understand the role of OH^- group of Cr, two different metadynamics simulations were performed. In both simulations, one of the metadynamics collective variables (CV1) was the coordination number of C_1 with the ring oxygen. In the case where the OH^- of the Cr^{+3}–OH^- group is not involved in ring opening (*cf.* Fig. 1), the other collective variable (CV2) was the coordination number of ring oxygen with respect to hydrogens in water molecules. This would allow the water mediated proton transfer to the ring oxygen. In the case where the OH^- of the Cr^{+3}–OH^- group facilitates glucose ring opening (*cf.* Fig. 2), the second collective variable (CV2) is the difference between coordination number of Cr^{+3}–OH^- oxygen atom and ring oxygen with respect to all hydrogens, including those of water molecules.

The free energy surface of the ring opening of glucose, without the involvement of the OH^- of the Cr^{+3}–OH^- is shown in Fig. 3. Even though Cr^{+3} remains coordinated to glucose, the pathway does not involve the protonation of Cr^{+3}–OH^- to form an additional water molecule on the metal center.

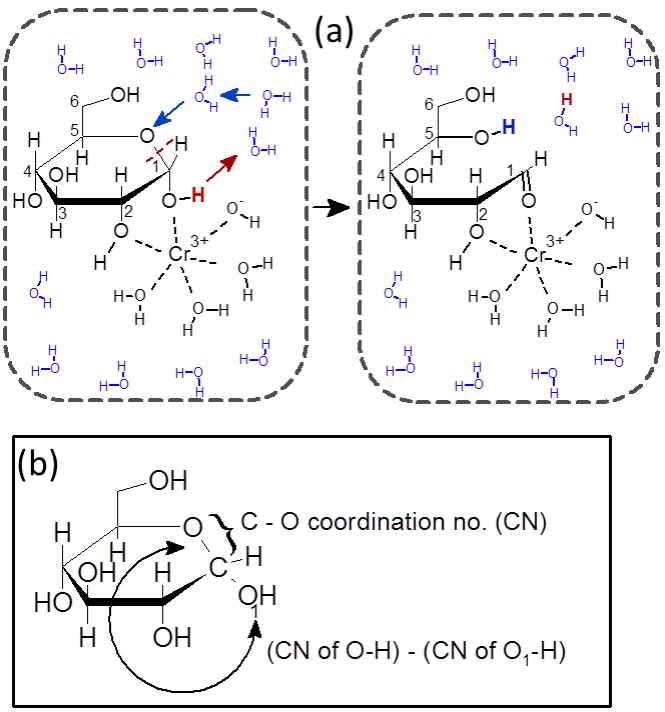

Fig. 1 a) Ring opening mechanism of glucose without the involvement of OH^- in Cr^{+3}–OH. **b)** Metadynamics collective variables implemented to simulate the ring opening.

The free energy barrier for this pathway (272 kJ/mol) is prohibitively high, thus strongly suggesting that Cr^{+3} alone or unhydrolysed $[Cr(H2O)4]^{+3}$ coordinated with glucose cannot catalyze the ring opening of glucose in water. It has to be noted that the metadynamics simulation was terminated shortly after the ring opening was observed.

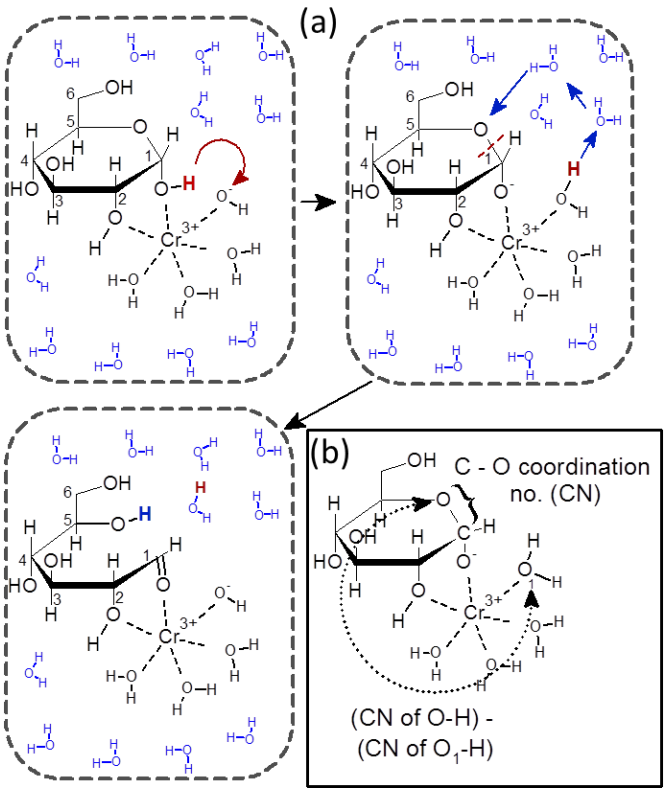

Fig. 2 a) Ring opening mechanism of glucose facilitated by the OH^- in the Cr^{+3}–OH^- group. **b)** Metadynamics collective variables implemented to simulate the ring opening.

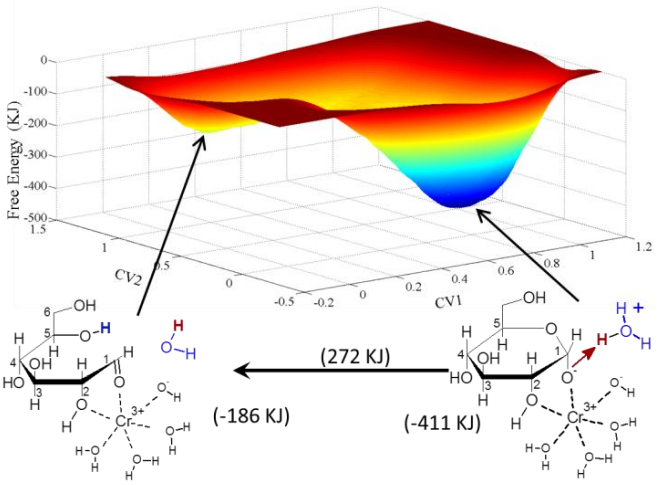

Fig. 3 Metadynamics calculated free energy landscape for the ring opening reaction of glucose without the involvement of the OH^- of the $[Cr(H_2O)_3OH]^{+2}$ group. Structures and free energy values at local minima are shown. The free energy barrier in the reaction step is shown over the arrow. Refer to Fig. 1(b) for the definition of collective variables CV1 and CV2.

The product free energy well was not allowed to fill completely, and hence, based on the difference in the free energies shown in Fig. 3, no conclusion can be drawn about the equilibrium of open vs. closed chain forms of glucose. A large difference in the free energy is however expected since more than 99.5% of glucose exists in the closed ring pyranosic form in water.

To further investigate the role of Cr^{+3}–OH^- in catalyzing the ring opening of glucose, a metadynamics simulation with a collective variable (CV2) taking into account the oxygen of the OH^- group on Cr^{+3}, i.e., allowing the formation of $[Cr(H_2O)_4]^{+3}$, was performed (*cf.* Fig. 2b). Fig. 4 shows the corresponding free energy surface. The free energy barrier for the ring opening, with $[Cr(H_2O)_4]^{+3}$ as an intermediate, is 125 kJ/mol. Comparison of the mechanisms shown in Fig. 1 and Fig. 2 and the corresponding free energy barriers in Fig. 3 and Fig. 4, respectively, clearly indicate that glucose ring opening may not proceed unless an intermediate state involving the protonation of the OH^- group on Cr ($[Cr(C_6H_{12}O_6)(H_2O)_3OH]^{+2}$ ➔ $[Cr(C_6H_{11}O_6)(H_2O)_4]^{+2}$), is formed.

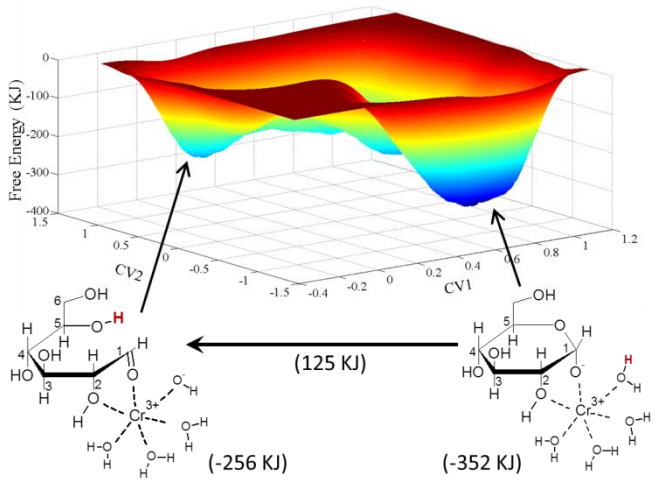

Fig. 4 Metadynamics calculated free energy landscape for the ring opening reaction of glucose, facilitated by the OH^- of the $[Cr(H_2O)_3OH]^{+2}$ group. Structures and free energy values at local minima are shown. The free energy barrier in the reaction step is shown over the arrow. Refer to Fig. 2(b) for the definition of collective variables CV1 and CV2.

Direct (or water mediated) transfer of proton from C_1 hydroxyl group to ring oxygen for ring opening is an extremely high barrier step and hence unhydrolysed Cr^{+3} would not be able to catalyze the ring opening and thus, the subsequent isomerization reaction. It has to be noted that since the initial deprotonation of glucose was observed in the CPMD equilibration period, the barrier for the same is not reported in the free energy surfaces shown in Fig. 3 and Fig. 4. However, an additional metadynamics simulation was performed to estimate the barrier and was found to be 79 kJ/mol.

To summarize, analogous to heterogeneously catalyzed glucose ring opening by the Sn–beta zeolite,[33] the partially hydrolyzed metal complex appears to be an active site in catalyzing the glucose ring opening reaction. The presence of the base OH^- on the Lewis acid center appears to play an important role in ring opening, in qualitative agreement with *ab initio* calculations.[33] The back donation of the proton to the ring oxygen of glucose to complete ring opening is mediated by water molecules in the immediate vicinity (but not in the inner coordination sphere) of the hydrolyzed metal complex.

Mechanism of Glucose Isomerization

The mechanism of the isomerization reaction is shown in Fig. 5. The isomerization reaction is initiated by the deprotonation of the open chain glucose molecule at C_2 carbon, followed by hydride transfer from C_2 to C_1 and back protonation at C_1 oxygen. The metadynamics collective variables implemented to simulate individual isomerization steps are defined in Fig. 6. Details are discussed below.

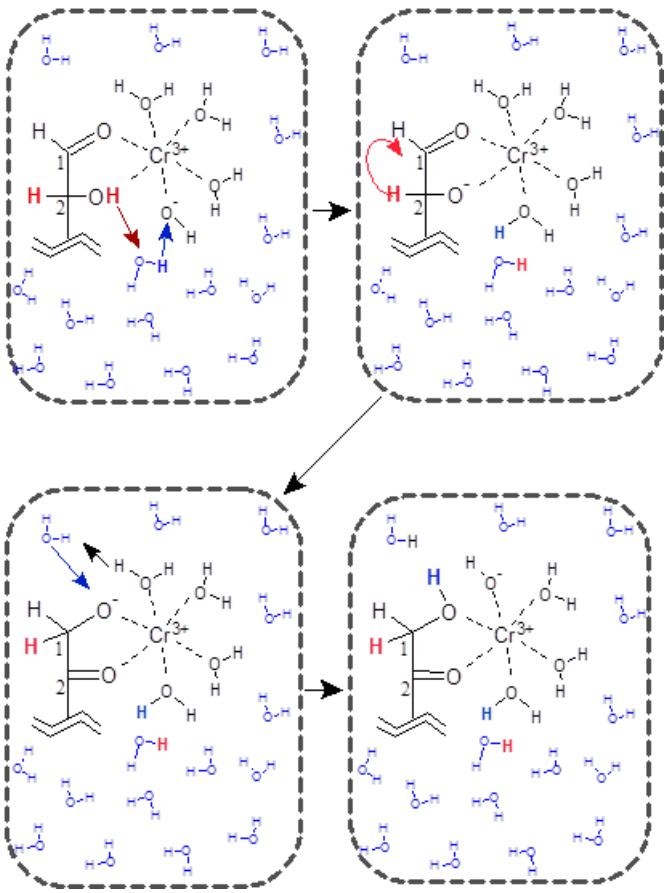

Fig. 5 Mechanism of isomerization of glucose, catalyzed by $[Cr(H_2O)_3OH]^{+2}$ in the presence of water molecules.

Deprotonation at C_2: The first step in the isomerization reaction is the deprotonation of C_2 hydroxyl group of the open chain glucose molecule. Based on our observation for the ring opening, it was believed that the presence of an intermediate $[Cr(H_2O)_4]^{+3}$ would be needed for the subsequent hydride transfer step from C_2 to C_1. One of the collective variables (*cf.* Fig. 6a) for the deprotonation step was the difference in the coordination of glucose oxygen and oxygen in Cr^{+3}–OH^-, with

respect to the hydrogen. However, since the orientation of the hydroxyl hydrogen of glucose is in the opposite direction of the metal complex, the C_2–O–H angle had to be incorporated as an additional collective variable (CV2). The free energy surface, as a function of these 2 collective variables is shown in Fig. 7.

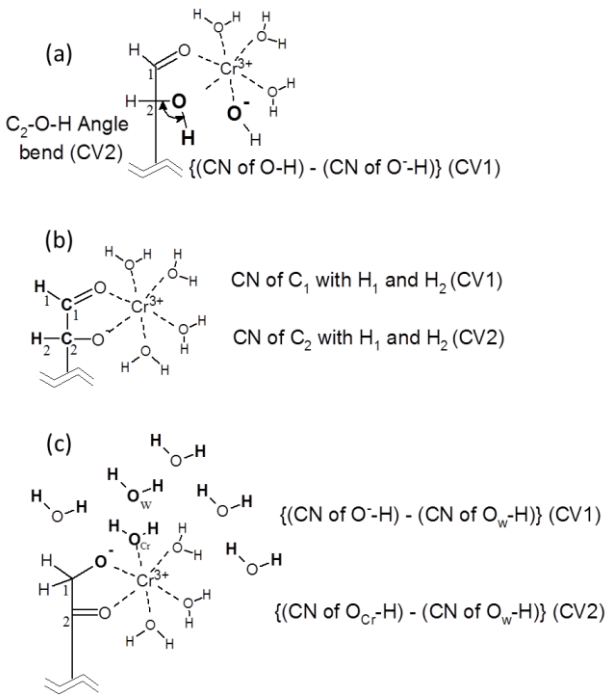

Fig. 6 Definition of collective variables (CV) for **a)** deprotonation, **b)** hydride shift, and **c)** back donation of proton. Atoms participating in CV definitions are shown in bold.

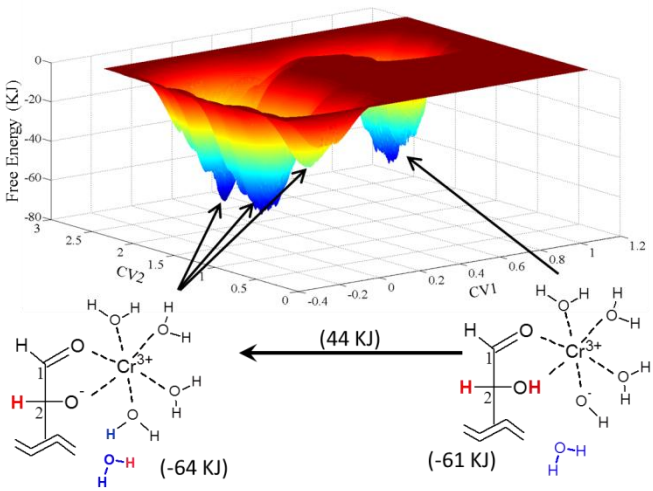

Fig. 7 Metadynamics calculated free energy landscape for the deprotonation of C_2 hydroxyl group of glucose. Structures corresponding to different minima in the free energy surface are shown. The free energy barrier in the reaction step is shown over the arrow. Refer to Fig. 6a for the definition of collective variables CV1 and CV2.

The deprotonation of glucose and protonation of Cr^{+3}–OH^- involves a free energy barrier of 44 kJ. It has to be noted that since the proton transfer from glucose oxygen to Cr^{+3}–OH^- is water mediated (similar to that for the closed ring glucose), the value of CV1 (*cf.* Fig. 7) goes from ~0.9 to ~0.1. If Cr^{+3}–OH^- would have picked up the same 'H' that was removed from the C_2 hydroxyl group, CV1 would have gone from ~0.9 to ~ –0.9. The water mediated proton transfer was also confirmed from the molecular dynamics trajectory. Since the hydrogen which was part of CV2 (angle bend) is picked up by a water molecule and the water molecule moves around in the simulation cell during the metadynamics simulation, several peaks at CV1 ≈ 0 (for different values of CV2) of approximately the same free energy level can be seen in Fig. 7. The free energy barrier between these peaks is 25–30 kJ/mol. With the proton transfer from C_2–OH to Cr^{+3}–OH^-, the average Cr–O distance for the C_2 oxygen decreases from ~2.1 Å to ~1.88 Å, thus making it more strongly coordinated with the metal center. The oxygen in Cr–OH, which now becomes Cr^{+3} ----- OH_2, on the contrary, moves slightly away from the metal center. The enhanced interaction of C_2 oxygen with the metal center is crucial for the next elementary step of isomerization, which is the hydride transfer from C_2 to C_1.

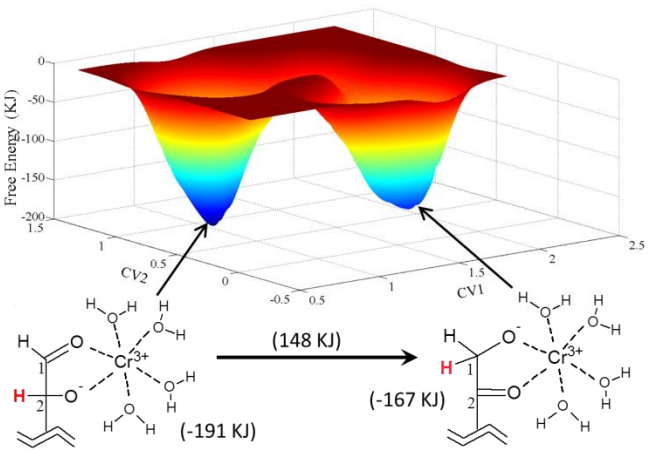

Fig. 8 Metadynamics calculated free energy landscape for the hydride transfer from C_2 to C_1. Structures corresponding to two minima in the free energy surface are shown. The free energy barrier in the reaction step is shown over the arrow. Refer to Fig. 6b) for the definition of collective variables CV1 and CV2.

Hydride Transfer from C_2 to C_1: Hydride transfer is usually the rate limiting step in sugars isomerization.[9,21,33-35] In the recent isotope labelling studies of glucose to fructose isomerization[21] using $CrCl_3$ and $AlCl_3$ as catalysts, a prominent kinetic isotope effect was observed when the deuterium was at the C_2 position, thus suggesting that hydride shift from the C_2 to C_1 position is the rate-limiting step with both catalysts. The implemented metadynamics collective variables to simulate the hydride transfer are defined in Fig. 6b. One hydrogen is bonded to each C_1 and C_2 before the hydride transfer and hence, CV1 ≈ CV2 ≈ 0.9. However, after the hydride transfer, CV1 is ≈ 1.8 and CV2

is ≈ 0.1. The Cr–O distance for the C_2 oxygen is ~1.88 Å and for the C_1 oxygen is ~2.1 Å before the hydride transfer, and the trend reverses after the hydride transfer. We believe that the presence of an intermediate water molecule on the metal complex after the deprotonation of open chain glucose ($[Cr(C_6H_{12}O_6)(H_2O)_3OH]^{+2}$ ➔ $[Cr(C_6H_{11}O_6)(H_2O)_4]^{+2}$) plays a key role in hydride transfer as well. This allows the Lewis acid metal center (Cr^{+3}) to have the strongest interaction with the C_2 oxygen (before the hydride transfer) and with the C_1 oxygen (after the hydride transfer) since C_1/C_2 oxygen is the only negatively charged oxygen in its inner coordination sphere. Since hydride shift in sugars isomerization is suggested to be a concerted transfer of neutral 'H' atom from C_2 to C_1 and of an electron from C_2 oxygen to C_1 oxygen,[36] a stronger interaction of the oxygen atom(s) with the metal center would enhance the catalytic activity of the metal center. The free energy surface for hydride transfer as a function of these collective variables is shown in Fig. 8. Hydride shift was observed to be an energetically slightly unfavourable step with a free energy barrier of 148 kJ/mol. Since hydride shift is shown to be the rate limiting step in the glucose isomerization reaction (with a free energy barrier higher than any other step)[33,34] in water,[37, 38] we compare the calculated free energy barrier with the experimental data.[11] The enthalpy of activation, as reported from the experimental data for glucose to fructose isomerization by $[Cr(H_2O)_3OH]^{+2,}$ is 64 kJ/mol.[11] Using the Eyring equation, if we plot the experimental kinetics data as $\ln(k/T)$ vs. $1/T$, the entropy of activation can be calculated from the intercept $[\ln(k_B/h + \Delta S/R)]$. The entropy of activation from the experimental data is –129 J/mol. Thus, at T=375 K the free energy of activation for $[Cr(H_2O)_3OH]^{+2}$ catalyzed glucose isomerization is 112 kJ/mol. The metadynamics calculated free energy of activation (148 kJ/mol) is significantly higher than the experimental value. We believe that the reason for this difference is that metadynamics simulations were performed with a few explicit water molecules, and do not fully account for the condensed phase environment effects. Hence, in order to fully account for the condensed phase reaction environment and to get an accurate estimate of the free energy barrier for the rate limiting step, we simulated the hydride transfer step in the presence of 124 explicit water molecules at the experimental density. The hydride transfer step, with the same metadynamics collective variables defined in Fig. 6b was simulated and the free energy surface is shown in Fig. 9. In the condensed phase environment, the hydride transfer step has a free energy barrier of 104 kJ/mol. This is in excellent agreement with the experimental value (112 kJ/mol) and indicates the important role of solvent in accurately estimating free energy barriers of these reactions. In comparison, the free energy barrier reported for hydride transfer catalyzed by the heterogeneous Sn–beta zeolite catalyst is 80 kJ/mol at 298 K.[33] The barrier for hydride transfer catalyzed by Cr (III) in ionic liquids ranges from 50–70 kJ/mol[39,40] and further reduces in the presence of two Cr (III) centres. However, in the present work, when we attempted to put two Cr (III) moieties to form a binuclear complex, similar to that in ionic liquids, one of the Cr (III) ions moved away from the glucose molecule upon relaxation. This indicates that, unlike ionic liquids, the hydride shift is probably catalyzed by a single Cr moiety in water and the cooperativity is created by the Lewis acid center, Cr, and base, OH.

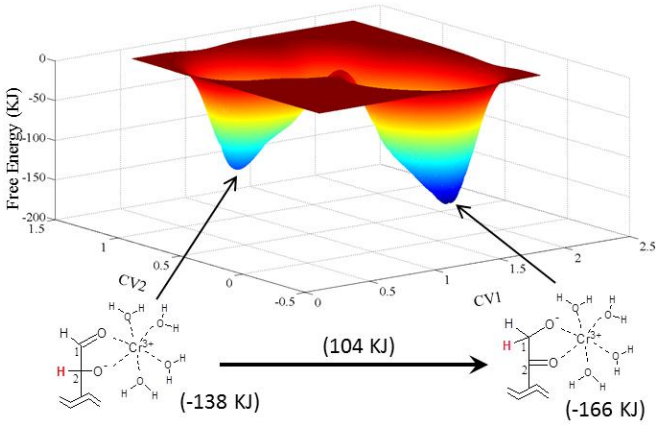

Fig. 9 Metadynamics calculated free energy landscape for the hydride transfer from C_2 to C_1 in a fully condensed phase. Structures corresponding to two minima in the free energy surface are shown. The free energy barrier in the reaction step is shown over the arrow. Refer to Fig. 6b for the definition of collective variables CV1 and CV2.

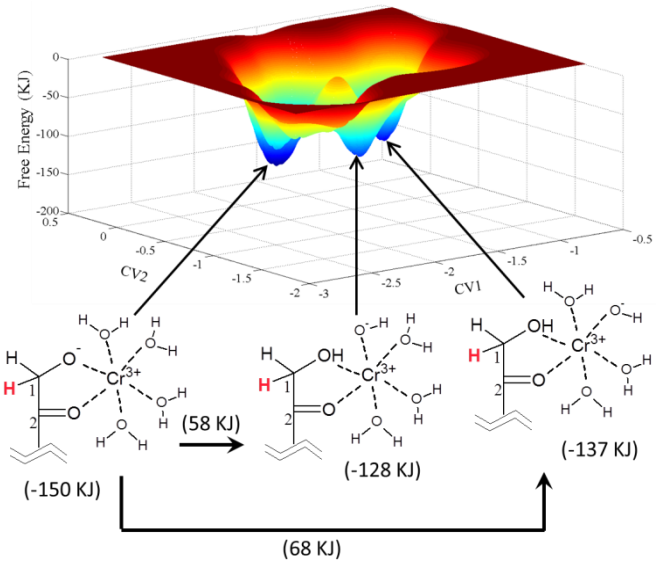

Fig. 10 Metadynamics free energy landscape for the reprotonation of the glucose molecule to complete the isomerization reaction cycle. Structures corresponding to minima in the free energy surface are shown. The free energy barrier in the reaction step is shown over the arrow. Please refer to Fig. 6c for the collective variables CV1 and CV2.

Reprotonation at C_1: The last step in glucose to fructose isomerization is the back donation of proton from the metal complex to the C_1 oxygen of the sugar. The collective variables implemented for this step are given in Fig. 6c. At the beginning

of the simulation, CV1 is equal to ~ –1.8 and CV2 is almost equal to zero. If the oxygen of the water molecule, which is coordinated with Cr^{+3} and is part of CV2, loses the proton for back donation (through water mediated proton transfer) to the sugar molecule, the final product state would have been CV1 ≈ –0.9 and CV2 ≈ –0.9. However, if any other water molecule that is not part of CV2 (but coordinated with Cr) gets deprotonated, then the final product would have CV1 ≈ –0.9 and CV2 ≈ –1.8. During the metadynamics run, both cases are observed and transfer of proton is always water mediated. The free energy barrier in the former case is 58 kJ and in the latter case is 68 kJ/mol (*cf* Fig. 10). Additionally, this step is energetically slightly unfavourable.

Conclusions

Car–Parrinello molecular dynamics simulations were performed for the first time to investigate glucose isomerization to fructose using $CrCl_3$ as a Lewis acid catalyst in water. Reactive events were captured using metadynamics and minimum energy pathways and corresponding free energy barriers were calculated. Coordination of glucose with partially hydrolyzed octahedral Cr(III) complex ($C_6H_{12}O_6$ + $[Cr(H_2O)_5OH]^{+2}$ ➔ $[Cr(C_6H_{12}O_6)(H_2O)_3OH]^{+2}$ + $2H_2O$) is required for catalyzing ring opening and isomerization reactions. Hydroxyl groups attached to C_1 and C_2 carbon atoms of glucose replace two water molecules in the inner coordination sphere of the metal. The OH^- group in the metal complex is in dynamic equilibrium with the rest of the three water molecules and has a stronger interaction with the metal center than that of the water molecules and glucose hydroxyl groups. The first step in isomerization is the deprotonation of glucose at one of the hydroxyl groups coordinated with the metal center, thus forming a glucose alkoxide type species with enhanced interaction between the metal center and glucose oxygen. This step is associated with a small free energy barrier. However, if the OH^- group attached to the metal complex does not pick up this proton to form an additional intermediate water molecule on the metal complex, the overall free energy barrier for ring opening becomes prohibitively high. With the formation of the intermediate water molecule, the free energy barrier for ring opening is significantly reduced. Similarly, for the isomerization reaction, the formation of this intermediate water molecule activates the hydride transfer. The intermediate water molecule later gives the proton back to the glucose molecule, via water mediated proton transfer and completes the isomerization reaction. This further solidifies our understanding that, in addition to the Lewis acid center, the attached OH^- Brønsted base is also essential for cooperative catalysis. Hydride transfer is the overall rate limiting step in glucose isomerization with a free energy barrier of 104 kJ/mol in good agreement with the estimated experimental free energy of activation of 112 kJ/mol.

Our simulations further support that $[Cr(H_2O)_5OH]^{+2}$ is the active species for glucose isomerization and that unhydrolysed, hexahydrated Cr cannot catalyze glucose ring opening and subsequent isomerization effectively. In addition, the mechanism for isomerization was detailed, and we found that the hydride transfer is the rate limiting step in the mechanism. Furthermore we have revealed the exact role of the OH^- group in the active species, which is to accept the proton from the hydroxyl group of glucose to form an intermediate water molecule and thereby to reduce the free energy barrier for ring opening and hydride transfer. Finally, we have shown the explicit participation of water molecules to mediate the proton transfers in the reaction cycle.

Acknowledgements

JJV and SHM would like to acknowledge financial support provided by Nanyang Technological University, Singapore. The authors would like to thank Dr. Vinit Choudhary, Dr. Stavros Caratzoulas, and Prof. Douglas Doren for useful discussions. DGV acknowledges support from the Catalysis Centre for Energy Innovation, an Energy Frontier Research Centre funded by the U. S. Department of Energy, Office of Science and Office of Basic Energy Sciences under award number DE-SC0001004.

Notes and references

[a] School of Chemical and Biomedical Engineering,
Nanyang Technological University,
62 Nanyang Drive,
Singapore, 637459, Singapore
Corresponding Author Email: shmushrif@ntu.edu.sg
[b] Center for Catalytic Science and Technology and Catalysis Center for Energy Innovation,
Department of Chemical & Biomolecular Engineering,
University of Delaware,
Newark, DE 19716, USA.

1 J. N. Chheda, G. W. Huber and J. A. Dumesic, *Angew. Chem. Int. Ed.*, 2007, **46**, 7164-7183.
2 M. J. Climent, A. Corma and S. Iborra, *Green Chem.*, 2011, **13**, 520-540.
3 H. Roper, *Starch-Starke*, 2002, **54**, 89-99.
4 J. N. Chheda, Y. Roman-Leshkov and J. A. Dumesic, *Green Chem.*, 2007, **9**, 342-350.
5 Y. Roman-Leshkov, J. N. Chheda and J. A. Dumesic, *Science*, 2006, **312**, 1933-1937.
6 A. I. Torres, P. Daoutidis and M. Tsapatsis, *Energy Environ. Sci.*, 2010, **3**, 1560-1572.
7 S. H. Bhosale, M. B. Rao and V. V. Deshpande, *Microbiol Rev*, 1996, **60**, 280-300.
8 A. Corma, L. T. Nemeth, M. Renz, S. Valencia, *Nature*, 2001, **412**, 423-425.
9 M. Moliner, Y. Roman-Leshkov and M. E. Davis, *Proc. Natl. Acad. Sci. USA*, 2010, **107**, 6164-6168.
10 Y. Roman-Leshkov, M. Moliner, J. A. Labinger and M. E. Davis, *Angew. Chem. Int. Ed.*, 2010, **49**, 8954-8957.
11 V. Choudhary, S. H. Mushrif, C. Ho, A. Anderko, V. Nikolakis, N. S. Marinkovic, A. I. Frenkel, S. I. Sandler and D. G. Vlachos, *J. Am. Chem. Soc.*, 2013, **135**, 3997-4006.

12 E. Nikolla, Y. Román-Leshkov, M. Moliner and M. E. Davis, *ACS Catal.*, 2011, **1**, 408-410.
13 S. K. Tyrlik, D. Szerszen, B. Kurzak and K. Bal, *Starch - Stärke*, 1995, **47**, 171-174.
14 A. A. Efremov, G. G. Pervyshina and B. N. Kuznetsov, *Chem.. Nat. Comp.*, 1998, **34**, 182-185.
15 C. B. Rasrendra, I. G. B. N. Makertihartha, S. Adisasmito and H. J. Heeres, *Top. Cat.*, 2010, **53**, 1241-1247.
16 Y. J. Pagán-Torres, T. Wang, J. M. R. Gallo, B. H. Shanks and J. A. Dumesic, *ACS Catal.*, 2012, **2**, 930-934.
17 S. De, S. Dutta and B. Saha, *Green Chem.*, 2011, **13**, 2859-2868.
18 L. Peng, L. Lin, J. Zhang, J. Zhuang, B. Zhang and Y. Gong, *Molecules*, 2010, **15**, 5258-5272.
19 D. Hiroishi, C. Matsuura and K. Ishigure, *Mineral Mag.*, 1998, **62A**, 626-627.
20 J. C. Bailar, H. J. Emléus, R. Nyholm, A. F. Trotman-Dickenson, A. Eds. *Comprehensive Inorganic Chemistry*; Pergamon Press, Oxford, 1973; Vol. **3.**
21 V. Choudhary, A. B. Pinar, R. F. Lobo, D. G. Vlachos and S. I. Sandler, *ChemSusChem*, 2013, **6**, 2369-2376.
22 CPMD, http://www.cpmd.org/, Copyright IBM Corp 1990-2008, Copyright MPI für Festkörperforschung Stuttgart 1997-2001.
23 R. Car and M. Parrinello, *Phys. Rev. Lett.*, 1985, **55**, 2471-2474.
24 W. Kohn and L. J. Sham, *Phys. Rev.*, 1965, **140**, 1133-1138.
25 N. Troullier and J. L. Martins, *Phys. Rev. B*, 1991, **43**, 1993-2006.
26 J. P. Perdew, K. Burke and M. Ernzerhof, *Phys. Rev. Lett.*, 1996, **77**, 3865-3868.
27 W. Humphrey, A. Dalke and K. Schulten, *J. Mol. Graphics Modell.*, 1996, **14**, 33-38.
28 M. Iannuzzi, A. Laio and M. Parrinello, *Phys. Rev. Lett.*, 2003, **90**, 238302.
29 A. Laio and F. L. Gervasio, *Rep. Prog. Phys.*, 2008, **71**, 126601.
30 A. Laio and M. Parrinello, *Proc. Natl. Acad. Sci. USA*, 2002, **99**, 12562-12566.
31 B. Ensing, A. Laio, M. Parrinello and M. L. Klein, *J. Phys. Chem. B*, 2005, **109**, 6676-6687.
32 A. Laio, A. Rodriguez-Fortea, F. L. Gervasio, M. Ceccarelli and M. Parrinello, *J. Phys. Chem. B*, 2005, **109**, 6714-6721.
33 R. S. Bermejo-Deval, R. S. Assary, E. Nikolla, M. Moliner, Y. Roman-Leshkov, S. J. Hwang, A. Palsdottir, D. Silverman, R. F. Lobo, L. A. Curtiss and M. E. Davis, *Proc. Natl. Acad. Sci. USA*, 2012, **109**, 9727-9732.
34 R. S. Assary and L. A. Curtiss, *J. Phys. Chem. A*, 2011, **115**, 8754-8760.
35 R. S. Bermejo-Deval, R. Gounder, M. E. Davis, *ACS Catal.*, 2012, **2**, 2705-2713.
36 V. Choudhary, S. Caratzoulas and D. G. Vlachos, *Carbohydr. Res.*, 2013, **368**, 89-95.
37 R. Xiong, M. Leon, V. Nikolakis, S. I. Sandler and D. G. Vlachos, *ChemSusChem*, 2014, **7**, 236-244.
38 M. Leon, T. D. Swift, V. Nikolakis and D. G. Vlachos, *Langmuir*, 2013, **29**, 6597-6605.
39 Y. Zhang, E. A. Pidko and E. J. M. Hensen, *Chem. Eur. J.*, 2011, **17**, 5281–5288.
40 E. A. Pidko, V. Degirmenci and E. J. M. Hensen, *ChemCatChem*, 2012, **4**, 1263–1271.